

# Optical and structural characterization of rapid thermal annealed non-stoichiometric silicon nitride film

Sarab Preet Singh<sup>1</sup>, P Srivastava<sup>1</sup>, G Vijaya Prakash<sup>1</sup>, M H Modi<sup>2</sup>,  
Sanjay Rai<sup>2</sup> and G S Lodha<sup>2</sup>

<sup>1</sup> Department of Physics, IIT Delhi, Hauz Khas, New Delhi-110 016, India

<sup>2</sup> X-ray Optics Section, Raja Ramanna Centre for Advanced Technology, Indore 452 013, India

E-mail: [prakash@physics.iitd.ac.in](mailto:prakash@physics.iitd.ac.in)

Received 27 February 2008, in final form 26 June 2008

Published 31 July 2008

Online at [stacks.iop.org/JPhysCM/20/335232](http://stacks.iop.org/JPhysCM/20/335232)

## Abstract

A detailed optical and structural characterization is carried out of a silicon nitride film deposited by a Hg-sensitized photo-CVD technique and subsequently subjected to rapid thermal annealing (RTA). An attempt has been made to correlate ellipsometry data with x-ray reflectivity (XRR) and x-ray diffraction data. Both the optical constants and density of the film were found to increase after thermal treatment. RTA treatment resulted in substantial change in the refractive index with more compaction of the film. This is explained in terms of hydrogen terminated defects/voids created due to predominant out-diffusion of hydrogen with RTA treatment.

(Some figures in this article are in colour only in the electronic version)

## 1. Introduction

Silicon optoelectronics has shown dramatic advances in the past decade as a potential commercially viable technology for optical communication, with the possibility of creating various optical modules such as interconnects, detectors and even potential sources [1–3]. However, issues such as substrate–layer interface problems and also lack of a complete understanding of processing artefacts are seen as technological bottlenecks. In current silicon-based technologies, rapid thermal processing (RTP) is now replacing conventional furnace processing for a range of processing steps [4]. The use of RTP is driven by the need to reduce the overall thermal budget associated with device fabrication, and in particular to maintain the desired device electrical properties. As the properties of the Si–dielectric interface and the bulk of the dielectric layer are central to the performance and long-term stability of devices, the influence of RTP on the properties of the Si–dielectric interface is an area that it is clearly important to characterize and understand. Rapid thermal annealing (RTA) is a process that is carried out after a film is deposited, usually at temperatures ranging from 800–1100 °C. At these temperatures, unwanted dopant diffusion can occur, especially in shallow implants. RTA minimizes unwanted diffusion by

utilizing short time, high temperature processing in which temperature is used as a switch to terminate the process step. In this type of processing, lattice repair will take place faster than diffusion. This results in minimization of various defects, which are normally present in dielectrics (SiO<sub>2</sub>, Si<sub>3</sub>N<sub>4</sub>, SiO<sub>x</sub>N<sub>x</sub>) deposited by chemical vapour deposition (CVD) techniques, such as plasma enhanced CVD and photo-CVD. Like all rapid thermal processes, RTA involves very short temperature ramp times and process cycle times. These cycles can range anywhere from nanoseconds to minutes. The short process cycle times and relatively high temperature may also induce structural changes in the dielectric films, which may result in modification of their refractive indices. Studies employing RTA [5–9] and/or exposure of dielectric films to light [10–12] to tailor their refractive indices are of great importance in optical waveguide applications to select appropriate material for core and cladding regions.

In the present work, we have studied the effect of RTA on silicon nitride film deposited by a Hg-sensitized photo-CVD technique. There are many studies available in the literature [5–9, 13] which discuss the effect of thermal annealing on optical, electrical and structural properties of silicon nitride films deposited on silicon. However, to the best of our knowledge, there are hardly any studies which correlate

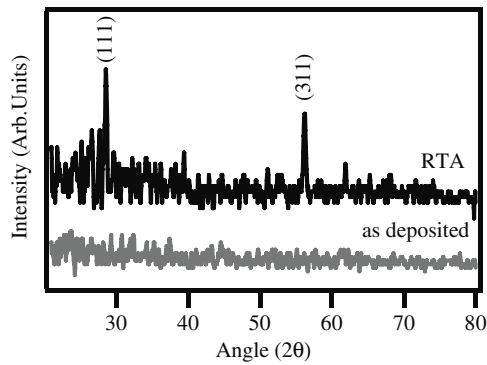


**Figure 1.** X-ray diffraction patterns of as-deposited and RTA silicon nitride films. Prominent peaks appearing in RTA treated films can be assigned to c-Si.

changes observed in the optical properties of these films with changes in their structural features on RTA treatment. In the present work, the changes observed in important optical parameters such as the refractive index are explained in terms of structural changes induced due to RTA.

## 2. Experimental details

Silicon nitride film was deposited on a p-type silicon (100) wafer by a Hg-sensitized photo-CVD method (Samco UVD10 model) using disilane (2% in Ar) and ammonia as reactant gases with a 2537 Å low pressure mercury lamp. The details of the photo-CVD system are discussed elsewhere [14]. The refractive index and thickness of the film were 1.95 and 360 Å ( $\pm 10$  Å), respectively, measured at 6328 Å with a Gaertner (model LII7) ellipsometer. The as-deposited sample was subsequently subjected to RTA in nitrogen ambient at 850 °C for 10 s. Glancing angle x-ray diffraction (GAXRD) measurements were carried out using a Philips Expert Pro-PW model 3040 with Cu K $\alpha$  ( $\lambda = 1.5418$  Å) radiation. To evaluate optical constants, namely the refractive index and extinction coefficient, spectroscopic ellipsometry was employed using a Sopra S-5 system to measure over the wavelengths from 250 to 900 nm with a glancing angle of 70°. Grazing incidence x-ray reflectivity (GIXR) measurements were performed to characterize the thin film structure for its thickness, roughness and density on both as-deposited and RTA samples, using Cu K $\alpha$  ( $\lambda = 1.5418$  Å) radiation with a home-made reflectometer [15]. Two slits of width 0.1 and 0.05 mm were used in a combination to generate the incident beam of 0.025° divergence. A razor blade was kept close to the sample surface to further reduce the beam size. Soller slits with 0.4° divergence were used in the incident beam to control axial divergence. The reflected beam was analysed by a graphite crystal monochromator followed by a scintillation detector. Electron density profiles (EDP) from the GIXR data were extracted using the well-known recursive formalism, in which the total thickness of the film was divided into 'n' small slices [16].

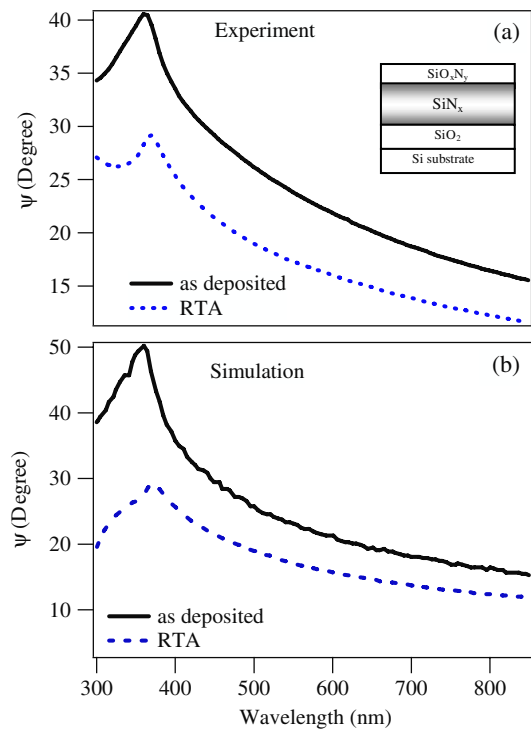


**Figure 2.** Ellipsometry analysis: (a) ellipsometer parameters  $\psi$  experimental and (b) simulations for as-deposited and RTA films. The inset shows a schematic representation of the three-layer model used in ellipsometry and XRR analysis (see text).

## 3. Results and discussion

Both as-deposited and RTA films were characterized by means of GAXRD, ellipsometry (single wavelength and white light) and GIXR techniques. X-ray diffraction patterns show that the as-deposited sample is completely amorphous in nature, while the RTA sample starts to show some crystallinity (see figure 1). The prominent diffraction peaks observed at  $2\theta$  values 28.27° and 56.02° in the diffraction pattern could be assigned to crystalline silicon of (111) and (311) planes, respectively.

Ellipsometry angles ( $\psi$ ,  $\Delta$ ) are recorded over the wavelength region 250–900 nm for the samples before and after RTA. Angles  $\psi$  and  $\Delta$  are obtained from the relation of the Fresnel reflection-coefficient ratio  $\rho = R_p/R_s = \tan \psi \exp(i\Delta)$  where  $R_p$  and  $R_s$  are reflection of light from p and s polarized light, respectively. These angles were fitted using the Marquardt–Levenberg minimization technique [17] to derive the optical constants, refractive index ( $n$ ) and extinction coefficient ( $k$ ). A better agreement between the experimental and simulated data was found when a three-layer model (see inset of figure 2) was assumed rather than a simple single-layer assumption. Adoption of a three-layer model can be justified as follows. The silicon oxide ( $\text{SiO}_2$ ) layer, just above the substrate, could possibly be due to the presence of native oxide prior to the deposition, while the existence of top oxy-nitride ( $\text{SiO}_y\text{N}_x$ ) layer could be understood from the fact that the sample was exposed to the atmosphere prior to measurements. The fitting parameters thus obtained from the fitting are shown in table 1. A reasonable agreement

**Table 1.** Relevant parameters, refractive index ( $n$ ), extinction coefficient ( $k$ ) (at  $\lambda = 6328 \text{ \AA}$ ) and thickness ( $t$ ) obtained from ellipsometric analysis. Respective layers are schematically represented in the inset of figure 2(a).

Layer (from substrate)	As-deposited film $n, k, t$ ( $\text{\AA}$ )	Rapid thermal annealed film $n, k, t$ ( $\text{\AA}$ )
SiO <sub>2</sub>	1.45, 0, 50	1.45, 0, 42
SiN <sub>x</sub> (EMA-3 layer)	1.98, 0, 282	2.36, 0, 197
SiO <sub>y</sub> N <sub>x</sub>	1.88, 0, 50	1.88, 0, 39

could be seen between experimentally obtained ellipsometry angles and the simulations from figures 2(a) and (b). The interface oxide (bottom) and oxy-nitride (top) layer thicknesses are very small (typically between 39 and 50  $\text{\AA}$ ) and more or less constant even after RTA treatment. The composition of the intermediate layer is obtained by Bruggeman’s three-component effective-medium approximation (EMA-3). The ambiguous values of refractive index and thickness obtained from single-wavelength (6328  $\text{\AA}$ ) null ellipsometry are used as verification through out the fitting process. The best fits were obtained for the intermediate layer combinations used in EMA-3 containing silicon oxy-nitride, hydrogenated silicon nitride, excess silicon and voids ( $\epsilon = 1$ ). Typical optical constants ( $n$  and  $k$ ) for respective components were used from the available literature [18]. As compared to the as-deposited film, the RTA silicon nitride film shows a substantial increase in the contribution of excess Si (from 16% to 28%) and voids (from 0 to 8%). Therefore our optical studies suggest the presence of excess Si in both as-deposited and RTA silicon nitride films. In addition, GAXRD measurements clearly show that at least some of the excess Si gets crystallized on RTA.

From the fits of ellipsometry angles, we eventually obtained the optical constants, namely refractive index ( $n$ ) and extinction coefficient ( $k$ ), over the wavelength region 250–900 nm for as-deposited and RTA treated silicon nitride film (see figure 3(a)). The refractive index and extinction coefficients of RTA film show significant enhancement compared to as-deposited film. For a comparison, the value of the refractive index increased from 1.98 to 2.36 (at 6328  $\text{\AA}$ ) after RTA. Moreover, the extinction coefficients show a clear rise in the edge at about 400 nm upon thermal treatment, which is insignificant in as-deposited film. A similar signature is also seen in refractive index profile, which is closely associated with c-Si optical features. Crystalline silicon and silicon nitride optical constants, available from [18], are also plotted in figure 3(b) for comparison. Such a substantial increase in the refractive index is attractive for optoelectronics, where refractive index contrast is one of the essential requirements, particularly for waveguide-based devices [19, 20]. However, it is to be noted that the ellipsometry data were taken and analysed to determine the optical constants and thicknesses by incorporating the data of available bulk values. Also, ellipsometry does not provide any quantitative information about the specific details such as hydrogen content and Si–H bonding.

Therefore, we further extended our investigations to understand the interfaces and structural properties found with

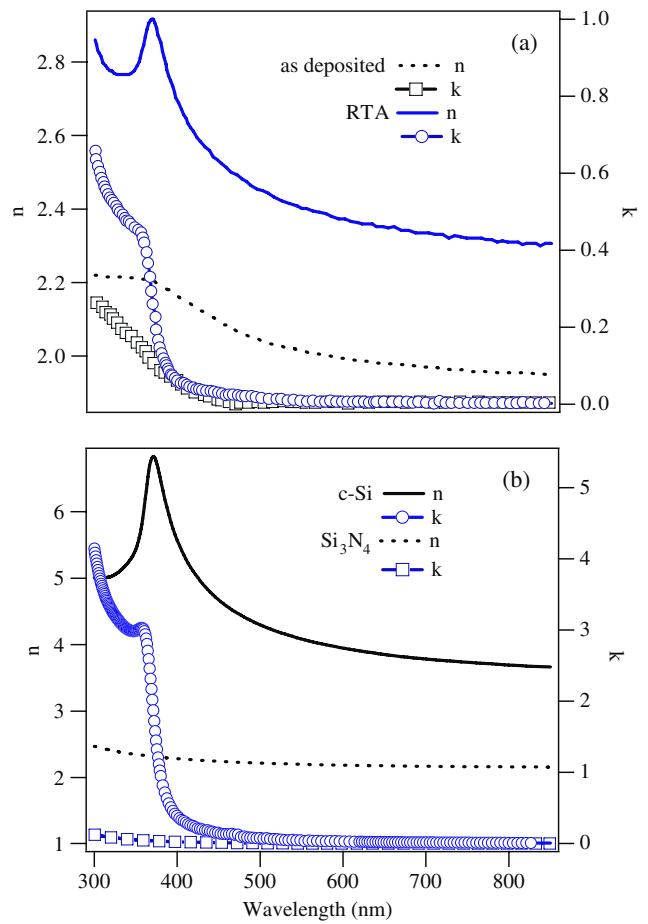


**Figure 3.** Plots of refractive index and extinction coefficients of (a) as-deposited and RTA films and (b) for c-Si and Si<sub>3</sub>N<sub>4</sub>, taken from [18].

GIXR measurements for both as-deposited and RTA films (see figure 4(a)). Electron density profiles (EDP) of the film before and after RTA obtained from the fit of reflectivity data are shown in figure 4(b). The following observations can be made from EDPs of as-deposited and RTA films (see figure 4(b)). For a clear understanding of the figure, it has been divided into three regions.

- (i) It is evident from region 2 (see figure 4) that the as-deposited film shows uniformity across the depth except near the air/film interface and film/substrate interface, whereas in RTA treated film the silicon nitride film shows substantial increase in EDP (in a certain portion), and also the profile is not as uniform as in the case of as-deposited film. The average value of density was found to increase from  $1.9 \text{ g cm}^{-3}$  (as-deposited) to  $2.44 \text{ g cm}^{-3}$  (on RTA). However, it is clear from the EDP profile of RTA film that density increment, and hence compaction, is taking place in only a certain portion (region 2). The reason for an increase in density of the film, after RTA, could be the evolution of hydrogen. The presence of hydrogen in the as-deposited film could possibly be due to the use of Si<sub>2</sub>H<sub>6</sub> and NH<sub>3</sub> as the initial reactant gases.
- (ii) A careful analysis of EDP profiles suggests that even after RTA a significant amount of hydrogen is probably

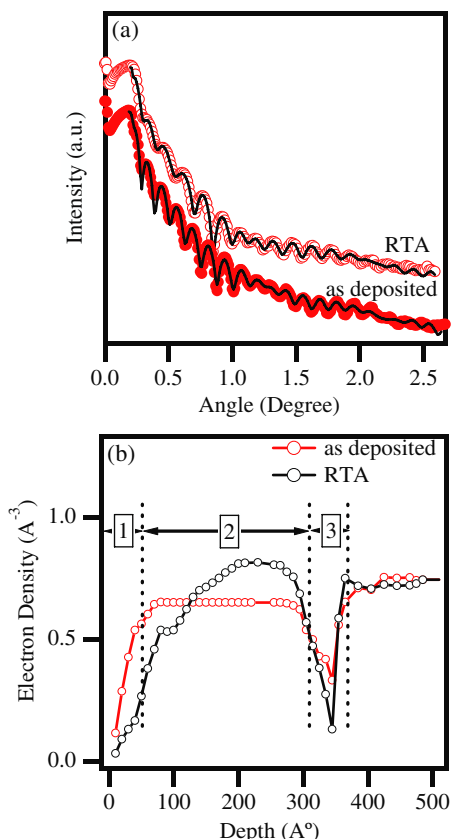


**Figure 4.** (a) GIXR spectra of as-deposited and RTA samples measured using  $\lambda = 1.5418 \text{ \AA}$  are shown along with fitted curves (continuous line). (b) The electron density profile obtained from the fit for as-deposited and RTA film. The three regions shown are described in the text.

still entrapped in the film. This can be appreciated by comparing regions 1 and 2 (see figure 4) of both as-deposited and RTA films. In the RTA film, trapping of hydrogen near the surface has probably caused a reduction in surface density with a thickness swelling. In the as-deposited sample, the density near the surface changes relatively faster than that of in the RTA film. In addition, region 3 in figure 4(b) suggests that we cannot rule out a small amount of hydrogen in-diffusion (towards the substrate). This is indicated by lower values of density (deepening of EDP) on RTA.

Combining ellipsometry and x-ray reflectivity (XRR) suggests that RTA treatment of the deposited silicon nitride film significantly enhances the density and optical constants. The reduction in the thickness of the film on RTA, as shown in the aforementioned ellipsometry analysis, is not so apparent from XRR analysis. However, both ellipsometry and XRR analysis show densification of the film on RTA. Such a significant enhancement of density could possibly be due to phase-separated c-Si with the elimination of broken silicon-hydrogen bonds in our silicon rich film. This eventually justifies our taking voids and c-Si to fit the aforementioned ellipsometry data and is also evidenced from the GAXRD data. Such phase separation in the films could possibly be

due to out-diffusion of hydrogen present in the as-deposited film. The hydrogen therefore predominantly evolves from the film. However, after RTA, signatures of a significant amount of hydrogen entrapment and hydrogen in-diffusion can be seen from the present GIXR data.

Though our present study, and the respective models used, does not explicitly take into account incorporation of hydrogen in the silicon nitride film, to verify the hydrogen evolution we have performed elastic recoil detection analysis (ERDA) on as-deposited and RTA silicon nitride films using  $100 \text{ MeV Ag}^{7+}$  ions. Our preliminary analysis clearly indicates that, compared to as-deposited film, the total hydrogen concentration reduces on RTA treatment. Further analysis on hydrogen evolution is in progress and will be published elsewhere.

#### 4. Conclusions

The present study indicates that RTA can be used to tailor the optical/physical properties of silicon nitride, which are eventually useful in many optoelectronic device applications such as optically active Si-based waveguides. However, more detailed and elaborate studies are needed for complete optimization of the entire RTA process. In particular the increase of c-Si content in the RTA films is quite promising and would further pave the way for intense optical studies. It is also equally important to see if such phase-separated c-Si could shed any light on nucleation/growth of silicon nanocrystals in silicon rich silicon oxides under controlled conditions [21–23]. Here, it is specifically seen as important, because in light emission from silicon nanocrystals the participation of interface states of silicon borne out of bonding/broken bonding with oxygen/hydrogen is not yet unambiguously understood.

#### Acknowledgment

One of the authors (Sarab Preet Singh) is grateful to the Indian Institute of Technology Delhi (IITD) for providing financial support.

#### References

- [1] Pavesi L 2003 *J. Phys.: Condens. Matter* **15** R1169–96
- [2] Pavesi L and Lockwood D J 2004 *Silicon Photonics (Springer Topics in Applied Physics vol 94)* (Berlin: Springer)
- [3] Soref R A 1999 *Silicon Based Microphotonics: from Basics to Applications* ed O Bisi, S U Campisano, L Pavesi and F Priolo (Amsterdam: IOS Press)
- [4] Deshpande S V, Gulari E, Brown S W and Rand S C 1995 *J. Appl. Phys.* **77** 6534–41
- [5] Pei Z and Hwang H L 2003 *Appl. Surf. Sci.* **212/213** 760–4
- [6] Beshkov G, Dimitrov D B, Velchev N, Petrov P, Ivanov B, Zambov L and Dimitrova T 2000 *Vacuum* **58** 509–15
- [7] Liu Y, Zhou Y, Shi W, Zhao L, Sun B and Ye T 2004 *Mater. Lett.* **58** 2397–400
- [8] Martinez F L, del Prado A, Martil I, Bravo D and Lopez F J 2000 *J. Appl. Phys.* **88** 2149–51
- [9] Boehme C and Lucovsky G 2000 *J. Appl. Phys.* **88** 6055–9
- [10] Akazawa H 2002 *Appl. Phys. Lett.* **80** 3102–4
- [11] Kyuragi H 1996 *J. Vac. Sci. Technol. B* **14** 3305

- [12] Modi M H, Lodha G S, Srivastava P, Sinha A K and Nandedkar R V 2006 *Phys. Rev. B* **74** 045326
- [13] Andersen K N, Svendsen W E, Stimpel-Lindner T, Sulima T and Baumgartner H 2005 *Appl. Surf. Sci.* **243** 401–8
- [14] Agnihotri O P, Jain S C, Poortmans J, Szlufcik J, Beaucarne G, Nijs J and Mertens R 2000 *Semicond. Sci. Technol.* **15** R29–40
- [15] Rai S K, Tiwari M K, Lodha G S, Modi M H, Chattopadhyay M K, Majumdar S, Gardelis G, Viskadourakis Z, Giapintzakis J, Nandedkar R V, Roy S B and Chaddah P 2006 *Phys. Rev. B* **73** 035417
- [16] Parratt L G 1954 *Phys. Rev.* **95** 359
- [17] Tompkins H G and Gahan Mc 1999 *Spectroscopic Ellipsometry and Reflectometry* (New York: Wiley)
- [18] Farouhi A R and Bloomer I 1991 *Handbook of Optical Constants of Solids* ed E Palik (San Diego, CA: Academic)
- [19] Giorgis F, Pirri C F and Tresso E 1997 *Thin Solid Films* **307** 298–305
- [20] Giorgis F 2000 *Appl. Phys. Lett.* **77** 522–4
- [21] Vijaya Prakash G, Daldosso N, Degoli E, Iacona F, Cazzanelli M, Gaburro Z, Puker G, Dalba P, Rocca F, Ceretta Moreira E, Franzó G, Pacifici D, Priolo F, Arcangeli C, Filonov A B, Ossicini S and Pavesi L 2001 *J. Nanosci. Nanotechnol.* **1** 159
- [22] Iacona F, Franzó G and Spinella C 2000 *J. Appl. Phys.* **87** 1295–303
- [23] Cazzanelli M, Navarro-Urriós D, Riboli F, Daldosso N, Pavesi L, Heitmann J, Yi L X, Scholz R, Zacharias M and Gösele U 2004 *J. Appl. Phys.* **96** 3164–71